FNAL TD note TD-07-008
Febr. 13, 2007. The final version of the note posted May 09, 2007

Focusing Solenoid HINS_CH_SOL_02
Fabrication Notes and Test Results

C. Hess, F. Lewis, D. Orris, M. Tartaglia, I. Terechkine, T. Wokas

I. Fabrication Notes and Expected Performance

Although initially designed as a prototype lens without any correctors, this device has been later equipped with two (horizontal and vertical) corrector windings to meet updated requirements to the linac beam transport system. The main features of the focusing lens have been described in the pre-release note [1]. Although the main features of the solenoid design did not change, certain adjustments introduced during fabrication of the lens with the embedded corrector windings resulted in certain changes in the solenoid performance. First, addition of correction winding required some reduction in the length of the coil to allocate sufficient space for the correctors' ends. Second, similar to what was done in the case of the prototype #1 (HINS_CH_SOL_01, [2]), Formvar-coated 0.8 mm strand ("Ryuji" type) was used. The insulated strand diameter was 0.835 mm (comparing to 0.826 mm in the case of the test coils that used 0.808 SSC inner strand obtained through LBNL). Finally, as in the case of the prototype #1, the winding was not as straightforward as it was for the test coils, which used strand with 30 μm "single-build" ML (mylar) coating. For this coil, our attempts to make a regular winding did not fully succeed: the outer layers were wound stochastically. This changed the main coil outer diameter relative to the expected value.

The correction dipole windings (horizontal and vertical) were described in [3]. These windings were made using existing slots in the copper bobbin of the main coil of the solenoid made for better cooling of the solenoid winding. The transverse magnetic field of the corrector windings, calculated for 2D geometry, is ~730 G at 250 A; this is about what is needed to provide the required beam deflection if the effective length of the windings is 85 mm. There was no 3D modeling made for these windings because it was considered a demonstration model and it was decided to use different technique of winding correction dipoles that would be less time consuming (see [3] for details). Nevertheless, testing the prototype was considered important because test results would prove the whole concept of making the correction windings inside the solenoid.

Expected Performance

After making the required adjustments in the coil length, diameter and number of turns for the main and bucking coils, the winding data for the main coil became the following:

- Strand: 0.8 mm (bare diameter) Formvar-insulated strand (so-called "Ryuji"-type).
- coil I.D. is 55.2 mm
- coil O.D. is 97.5 mm
- Total turns - 2234
- coil length at I.D. - 74.0 mm
- compaction factor - 0.717, which is quite close to what the test coils (wound using SSC strand) had, and just slightly higher than what was used in the preliminary magnetic design (0.71).

The data for the two bucking coils are shown below. For both of them (#3 and #5) coated 0.6 mm Oxford 54-filament strand was used. There are 400 turns in each coil.

Coil	BC #3	BC #5
ID	53.2 mm	53.2
OD	97.0 mm	99.1 mm
L	6.47 mm	6.6 mm
Compaction Factor	0.798	0.747

During 3D ANSYS modeling of the longitudinal dynamics of the system [4], it was found that after cooling down, a gap can appear between the clamp flux return and bucking coils. The presence of the gap can result in coil movement and lead to quench. To compensate for contraction of the flux return during cooling down, a gap of ~ 0.55 mm was left between the flux return body and it's flange. An increased axial compression force of 4000 N was also used while assembling the device. After welding, the remaining gap was between 0.4 and 0.5 mm. The final assembly features are shown in Fig. 1 below.

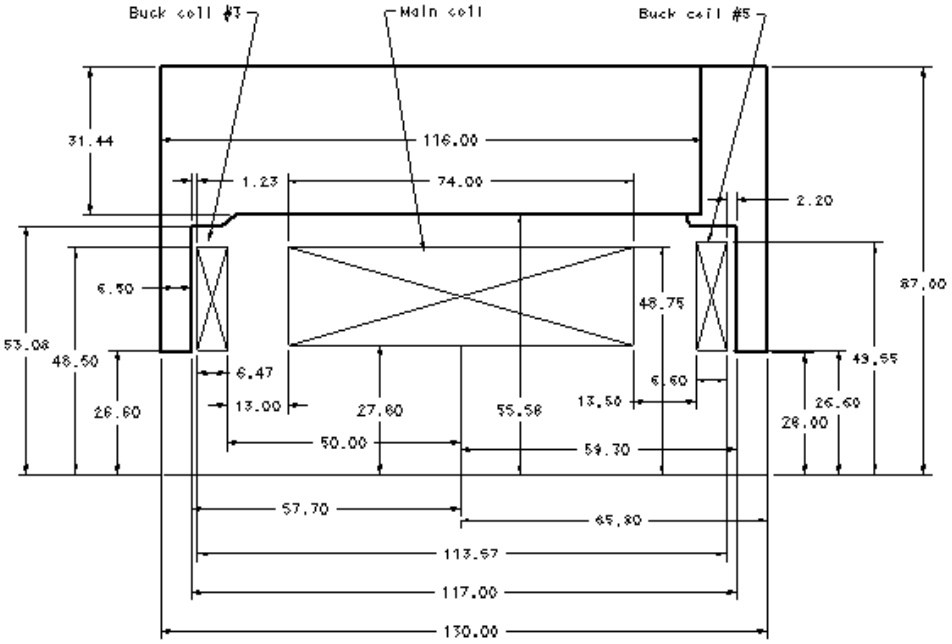

Fig. 1: HINS_CH_SOL_02 as built

To find the solenoid quench characteristics, we needed to know the strand critical surface: this has been measured in the TD SC material lab by E. Barzi and D. Turrioni using Teslatron. Tables 1 and 2 below present the measured critical current versus magnetic field at 4.2 K for the 0.6 mm strand used to fabricate the bucking coils and for the 0.8 mm main coil strand.

Table 1: Critical current versus magnetic field for 0.6 mm strand

B (T)	0	1	2	3	4	5	6	7	8
I (A)	978	722	546	457	392	334	275	210	140

Table 2: Critical current versus magnetic field for 0.8 mm strand

B (T)	5	6	7	8	9
I (A)	664	531	398	260	115

The expected longitudinal distribution of the magnetic field along the axis of the solenoid is shown in Fig. 2 for the case when the three coils are connected in series, and the transverse distribution of the magnetic field shown in Fig. 3. The peak transfer function at the center of the lens is 6.3/250=.0252 T/A.

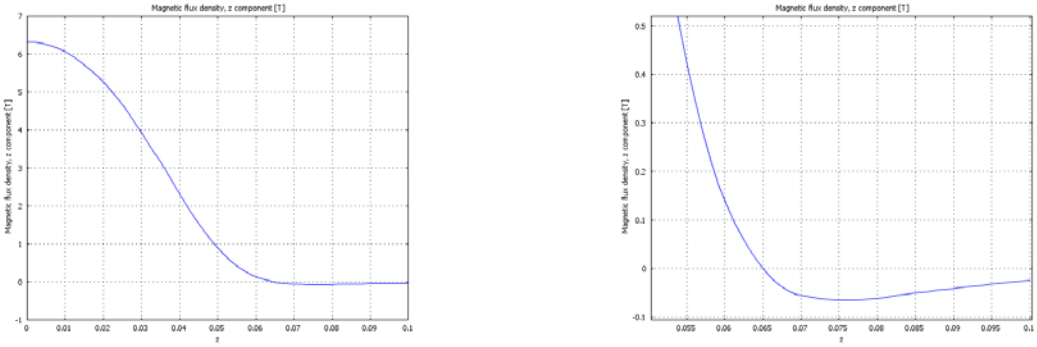

Fig. 2: B(z) at 250 A on the solenoid axis (r = 0).

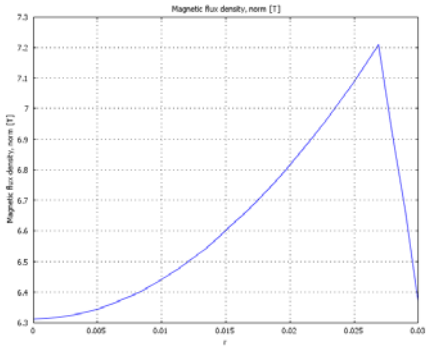

Fig. 3: B(r) at 250 A at the solenoid center (z = 0).

Quench behavior of the lens can be determined from Fig. 4, where the load lines intersect corresponding strand critical surfaces, for the main coil and bucking coil #3 (with the highest magnetic field of the two bucking coils), in the case with all three coils connected in series. The quench current of the bucking coils is slightly higher than that of the main coil. The maximum current is 275 A at 4.2 K. The quench parameters can be recalculated for the test temperature of 4.3 K, which result in the maximum current of ~ 270 A.

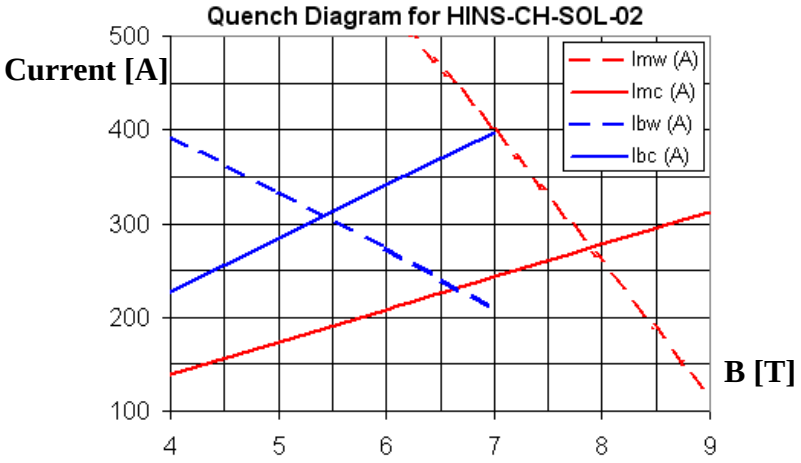

Fig. 4: Quench performance of the lens at 4.2 K with the coils connected in series.

The effective length of the solenoid is 70 mm. At 250 A, the squared field integral along the Z axis is 2.12 T^2m; this is higher than the 1.8 T^2m required to meet specification for the solenoid. The specification is met at 230 A and the lens still has a theoretical margin in current of ~ 15 % (the target design margin was about 20 %).

II. Performance Test Results

For this test the top plate of the stand 3 test Dewar was modified to install three pairs of current leads, in order to independently power parts of the lens. One pair was used for the main coil, the second pair for the two bucking coils connected in series, and the third pair for the two corrector dipoles connected in series. The test was made in stages: first, only the main coil was tested; then the two bucking coils connected in series were trained; after this, the main coil and the bucking coils were connected in series and the lens was tested to the maximum current that the power supply allowed; next, the corrector windings were tested to the maximal current of the power supply; finally the corrector windings were tested in the field generated by the lens. The nominal current of each one of two available power supplies was 250 A, but it was later found they could be operated safely and reliably even at 275 A. Training ramps were all made at 2 A/s.

1. **The current in the main coil (alone)** reached 260 A, having one intermediate quench at 250 A. We did not try to increase the current at this point because we did not have information on how the power supplies were protected.

2. **The bucking coils (alone)** required more training. The coils quenched at currents in the following sequence: 185 A – 195 A – 203 A – 208 A – 228 A – 241 A. Two subsequent ramps to 250 A were made (with 30 second flat-top) in which no quench occurred. We could not tell which of the bucking coils was quenching because there was not a voltage tap between the two coils (miscommunication problem).

3. **The main coil and the bucking coils in series** showed very quick training with only one quench at 187 A before reaching the current of 260 A. The quench happened in one of the bucking coils, which is demonstrated in Fig. 5 by the captured voltage growth on the bucking coils. The corresponding voltages on the parts of the main coil were negative, thus pointing to pure inductive nature of the signal due to the fact that the coil current declined after quenching. Premature quenching in the bucking coils was expected at this current (and field) level because the coils have been designed quite narrow in width, so they were flexible enough to move slightly under relatively high stress developed during the solenoid excitation (total force of ~ 70,000 N).

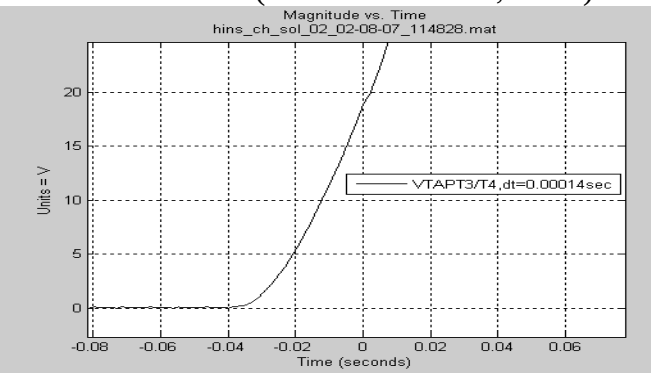

Fig. 5: Resistive voltage developed across the bucking coils at quench.

4. **Correction windings (alone)** did not quench up to the maximal current of 260 A. Neither of the correction windings quenched at 260 A when the current in the lens was set to 200 A and then to 250 A.

5. After the power supply protection details were resolved, the runs were made with the current in the main coil at the level 260 A. One quench in the main coil occurred when the current in the correction dipole reached 273 A. Repeated training cycles did not result in any increase or degradation of the quench current.

So, this prototype focusing lens with embedded correction dipoles successfully passed the performance test. The device meets specification for both correctors and the lens, with ~15 % margin in quench current.

III. Magnetic Measurements

The successful and quick performance test left plenty of liquid He to make thorough magnetic measurements. Magnetic measurements were made in a number of power configurations, using several different Hall probes. The probes, support and drive systems, and readout devices were utilized for previous test solenoid measurements. LabView readout was used to record the probes' voltages and positions, and precision Unix readout recorded magnet currents (see Table 1).

Table 1. Hall Probes and Digitizing Instruments for Magnetic Measurements

Probe Label	Probe Ser.No/ Bar Code	Instrument	Instrument Ser.No/Bar Code	Field Orientation wrt solenoid axis
A	BC 000833	Group3 DMT-141	BC 000801	1D, Parallel
B	BC 000829	Group3 DMT-141	BC 000801	1D, Transverse
C	SN 26-05	Keithley 2700	SN 899874	3D "old"
D	SN 54-06	Keithley 2700	SN 899874	3D "new"

For each of the solenoid power configurations (Main Coil only, Bucked Coils only, Main+Bucked Coils), the field strength versus position was measured along the solenoid axis using Probe A, at a fixed magnet current of 75A (the precise unix value was 74.68A). Fig. 6 shows the normalized (field/current) field profile of the Main Coil-only; the measured peak transfer function is 0.0305 T/A, and the predicted value is 0.029 T/A.

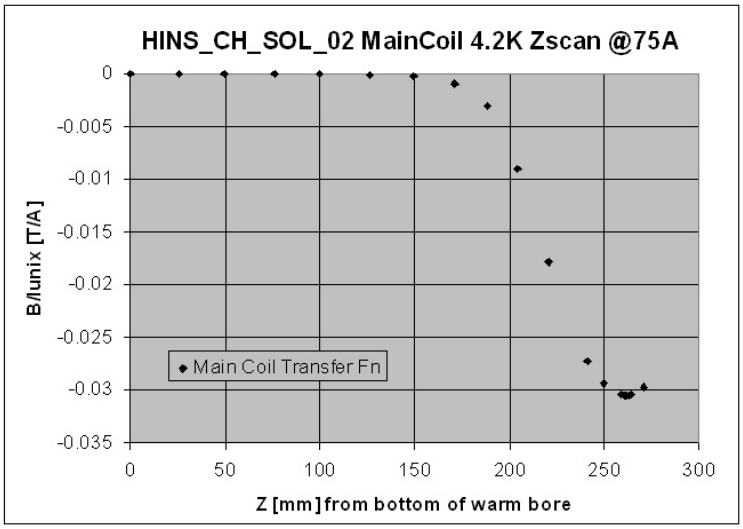

Fig. 6. Normalized field profile on solenoid axis for main coil-only powered.

In Fig. 7 the main coil-only and bucking coil-only field profiles at 75A are overlaid to show the relative sign and magnitude of their individual contributions, and the positions of the field maxima and minima (here the sign of B implies the main coil field was pointing up).

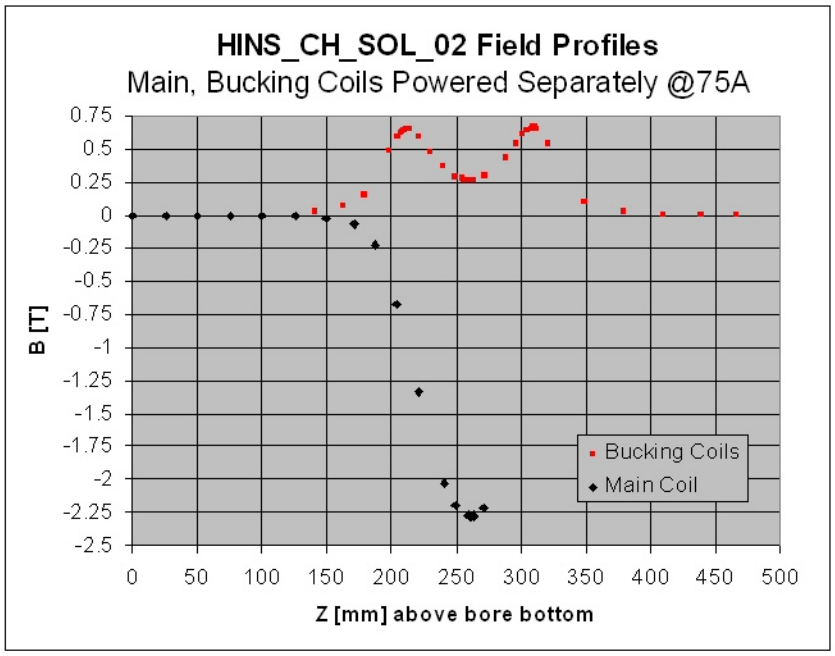

Fig. 7. Field strength versus position along the solenoid axis for main coil and bucking coils powered separately.

Fig. 8 shows the normalized field shape with both main and bucking coils powered at 75A, in which case the peak transfer function of 0.0269 T/A is slightly higher than the expected value, 0.0252 T/A.

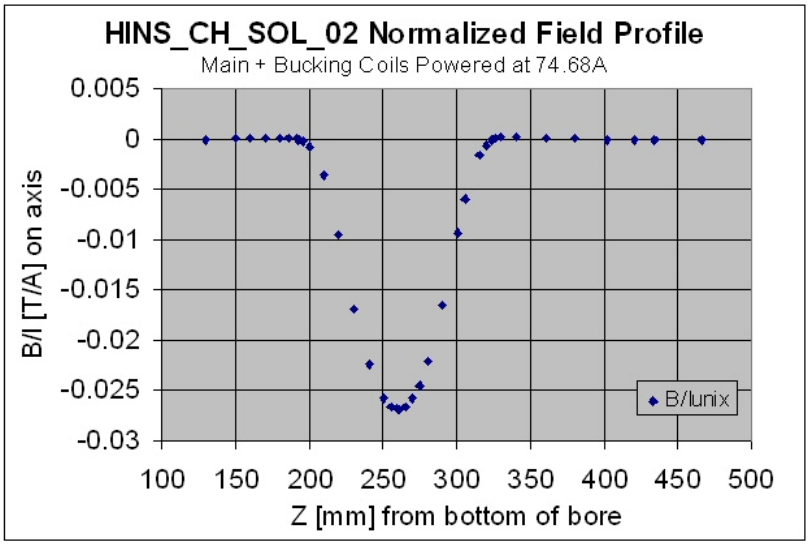

Fig. 8. Normalized field profile along the solenoid axis with main and bucking coils powered in series.

Fig. 9 examines the field strength versus position in the transition region between the main and bucking coils: in this magnet the bucking coils dominate in this region, with differing amplitude due to slight differences in the coil parameters. This graph should be compared with that in Fig. 2.

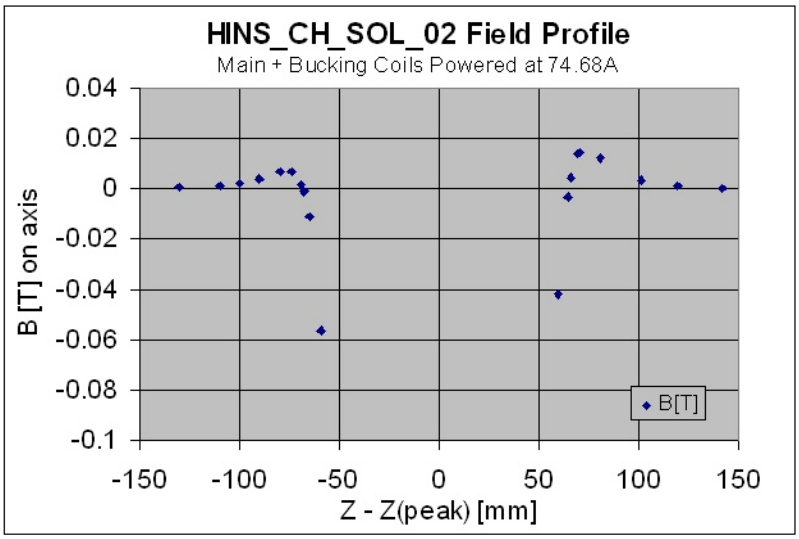

Fig. 9. Field strength versus position (relative to peak) along Main+Bucked coil powered solenoid, showing regions between coils are dominated by Bucking coil field.

Next, the probe B was installed on the axis, in the G10 support center position (Fig. 10), to measure the transverse field when the dipole corrector coils were both powered in series. It was positioned at the solenoid center and rotated to an angle that gave maximum field (thus measuring the vector sum of fields from these two orthogonal coils), which was 180 degrees according to the local angle-measuring system. With both correctors powered at 75A, the probe was scanned through the magnet to capture the longitudinal field profile, which is shown in Fig. 11.

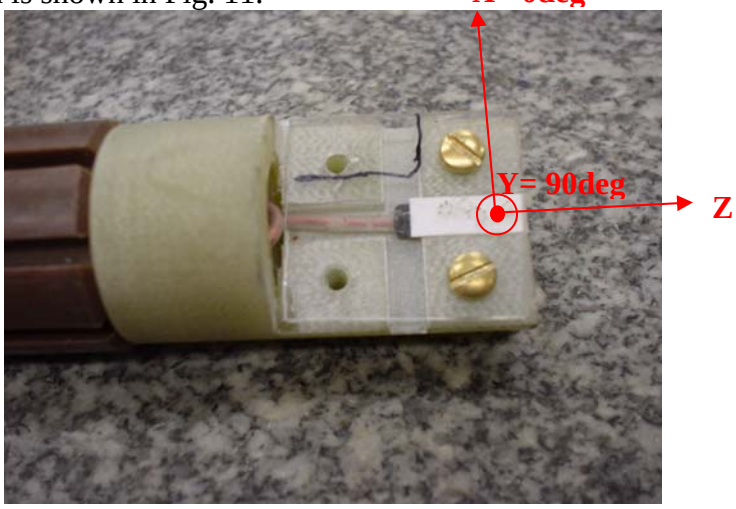

Fig. 10. Senis 3D Hall probe centered in probe support, with coordinate axes labeled; the 1D Hall probe was also placed in this position for transverse field measurements.

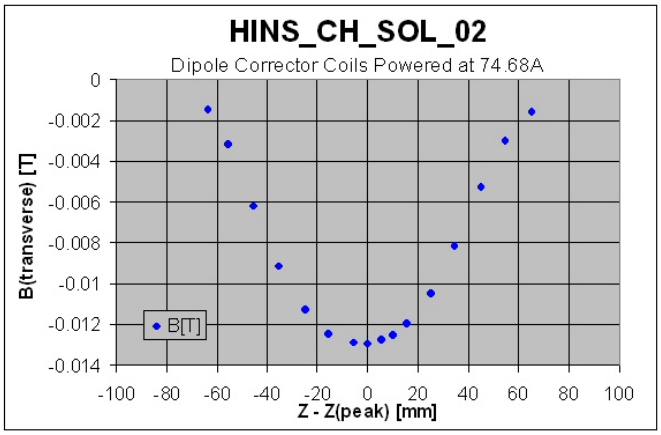

Fig. 11. Profile of transverse field strength versus position (Zpeak = 265.09mm) for dipole correctors powered in series at 75A

After corrector coil training, the angle scan at the solenoid center was repeated at 250A, shown in Fig. 12, confirming the peak field at 180 degrees.

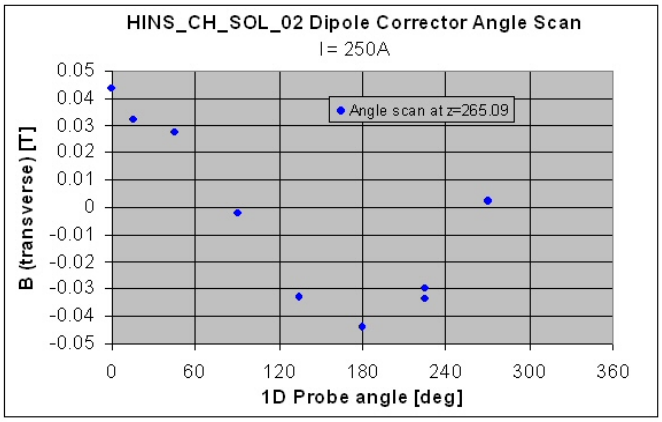

Fig. 12. Transverse field strength versus (approximate) angle, for dipole correctors powered in series at 250A at solenoid center position.

The peak transfer function of a single dipole corrector coil is found to be

$$B/I = 0.044 / 250 / \sqrt{(2)} = 0.000124 \text{ T/A},$$

which is in reasonable agreement with the expected value 0.000146 T/A [3] for a long coil. The dipole field profile in Fig. 11 fits to a parabola reasonably well:

$$B(z)/ I = -1.667*10^{-4} +3.547*10^{-8}\cdot z + 3.86710^{-8}\cdot(z)^2$$

where z is the distance from solenoid center, **in millimeters**. Integration from -65 to 65 mm gives an **integral strength for one dipole** (thus dividing by $\sqrt{(2)}$) at 250A of ~0.25 T-cm. This bending strength is about what is required for the room temperature (CH) section of the front end linac.

After the quench performance studies were completed, Probe C was installed in the G10 support, center position (see Fig.10) to map the three field components versus position along the solenoid axis with all the three coils powered at 250A. First the probe was moved to the peak field position and an angle scan in 45 degree steps (Fig. 13) was made to determine the angle at which corrector dipoles were aligned with the X and Y axes of the probe.

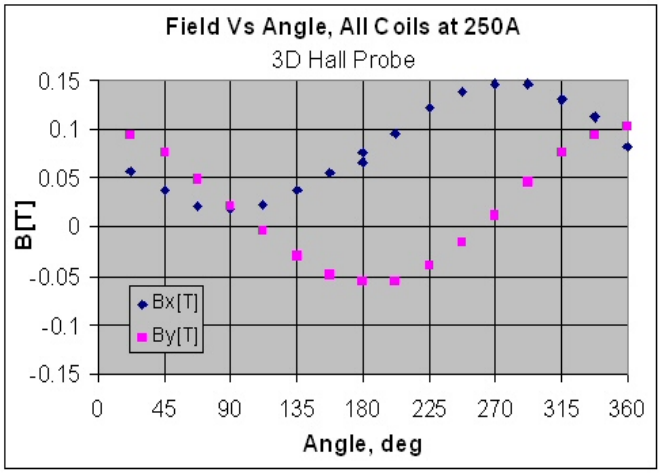

Fig. 13. 3D Hall probe angle scan at solenoid center position with all coils powered.

This angle marked on the probe shaft was 135°. Fig. 10 shows the three axes of the Hall probe and corresponding shaft angles for the X and Y field directions. Fig. 14 shows a drawing of the corrector dipole coils, with the 135° line translated from the magnet to the shaft during assembly. To summarize, we have a known relationship between the X and Y probe orientation relative to the dipole corrector planes.

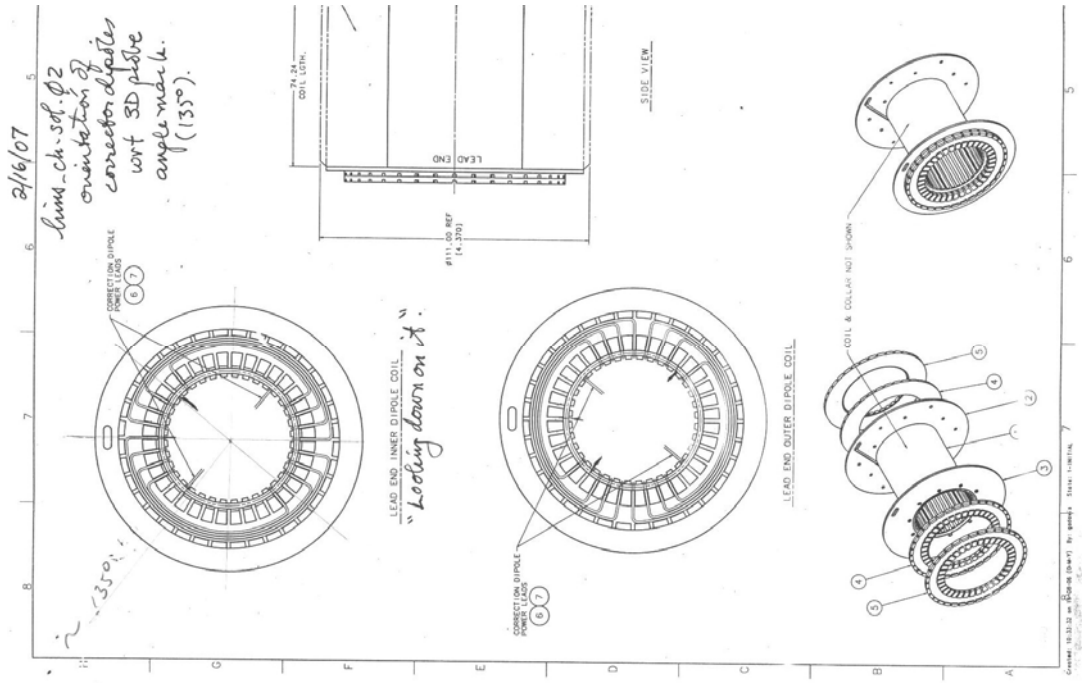

Fig. 14. Orientation of corrector coils with respect to the probe angle mark.

With the probe set at this 135 degree angle, a scan was made along the solenoid axis to measure all three field components versus position, in order to begin to understand alignment issues. It should be noted that the G10 shaft and probe support used were the same as used in previous test solenoid and high field magnet calibration studies: the long shaft had one centering bearing just above the actual probe holder. *[In the test of HINS_CH_SOL_01 that followed, a second bearing was added about 6 inches higher, to*

try and provide "local" centering in case the long shaft might introduce a probe tilt]. The Z-scan measurements with all coils powered is shown in Fig. 15. At this point we expected to see the Bz component of the main field on the Z probe, and (because the probe is inserted along the axis) not to see other two ("radial") components of the main coil field. X and Y probe should give instead a sine-type profile associated with the corrector field. Instead we saw quite a different reading on the Y-probe.

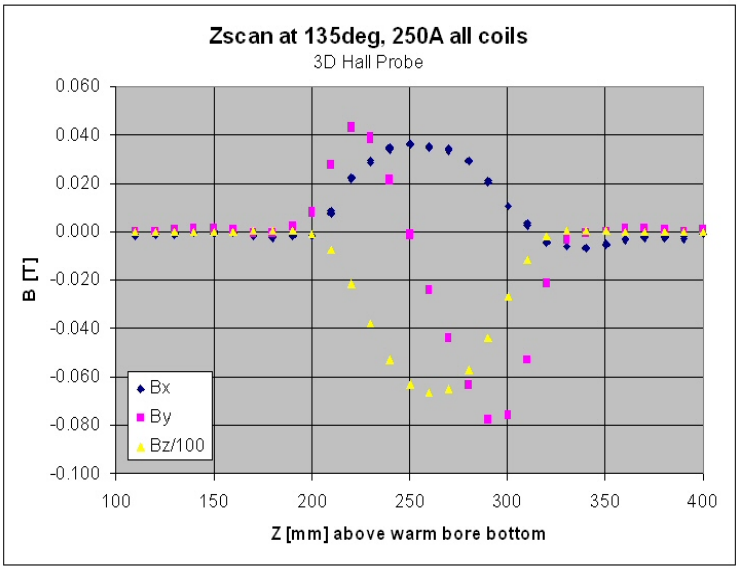

Fig.15. Field strength along solenoid axis with 3D probe oriented along corrector dipole directions, with all coils powered.

This result led us to repeat the Z-scan separately with the Main+Bucking coils-only powered (Fig. 16), and again with the dipole correctors-only powered (Fig. 17), in order to distinguish the contributions from tilts and offsets of the probe and/or warm bore relative to the solenoid axis, from the 3D shape of the dipole corrector field.

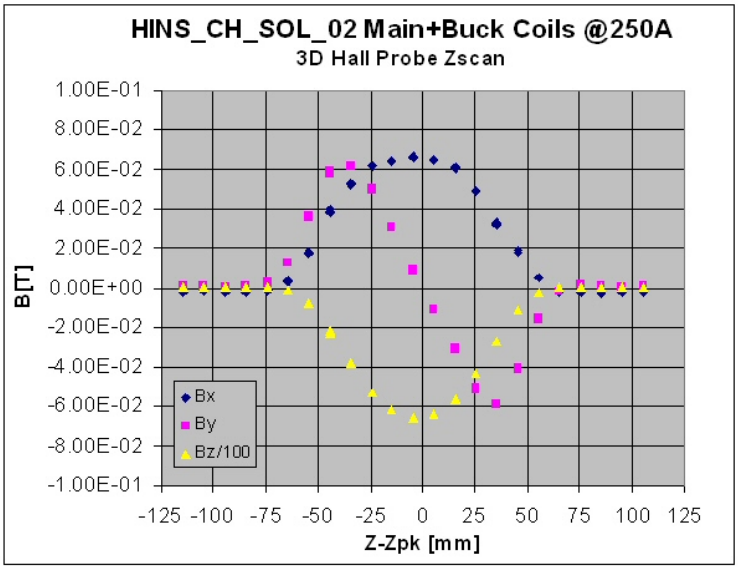

Fig.16. 3D field strength versus position for Main+Bucking coils only powered.

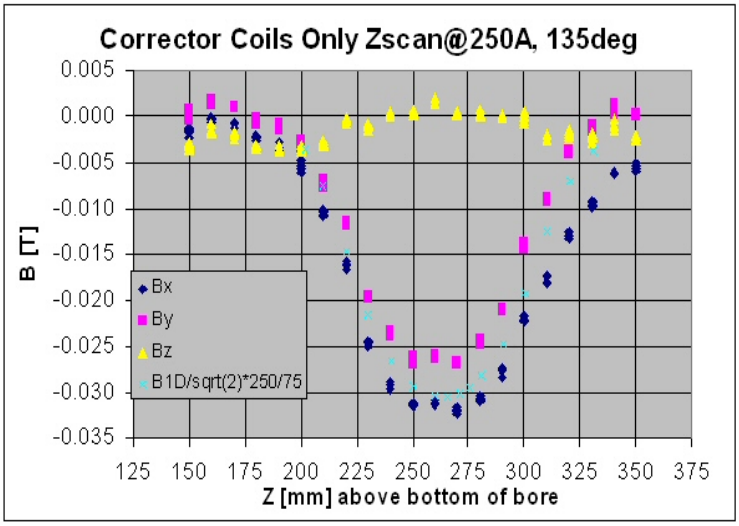

Fig. 17. 3D field strength along the solenoid axis with only dipole corrector coils powered. The yellow triangles indicate the level of z-component at the coil ends.

In Figure 16, one can see that B_x is approximately 1% of the main field, B_z, which could be explained by a small tilt of the probe in the xz plane, $\sin\alpha = \alpha = 0.01$. B_y can be explained by an offset of the probe from the solenoid axis: Fig. 18 shows the predicted B_y field profile (from Opera2D calculation of the DTLv6a bucked coil solenoid at 188A), along a line parallel to the solenoid axis but with a small radial offset (0.1mm) – the shape agrees with the measured shape of B_y.

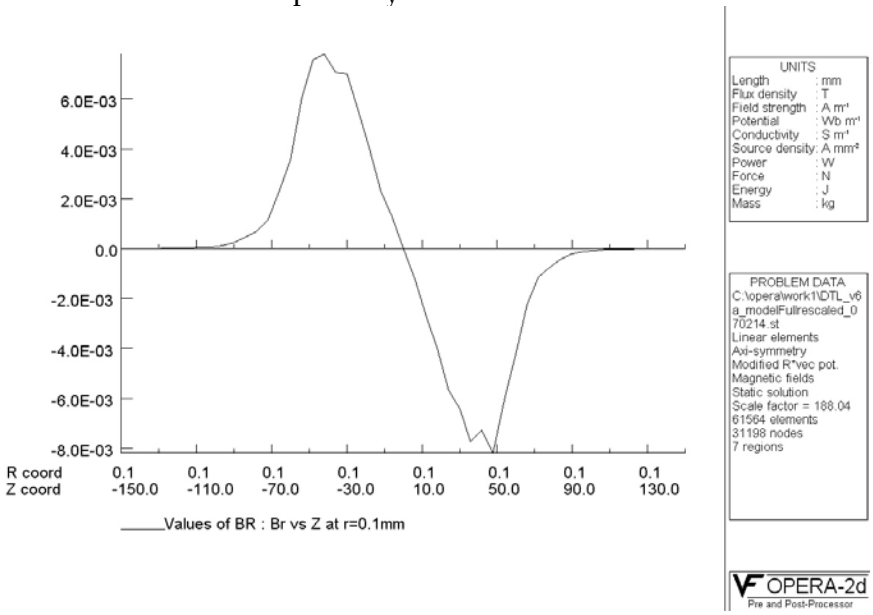

Fig. 18. Radial field (at 188A) strength versus Z at off axis position, r = 0.1mm

Fig. 19 shows the peak B_y, normalized to the peak axial field $B_{z\,peak}$, as a function of the offset: the data in Fig. 16 give $B_y/B_{z\,peak} = .06/6.57 = 0.0091$, which graphically (Fig.19) translates to an offset of the axis in the "y" direction of about 0.065 mm. Subsequent study of the probe holder reveals that there is indeed an offset in the Y direction of the Hall probe element from the center line: in Fig. 20 a drawing of the probe

holder shows the probe reference plate surface is offset by .036 inches (= .91 mm) above the center line of the support; according to the specification sheet, the Hall probe element is 1.5mm below this level, which puts it 0.59 mm below the center line. This is in reasonably good agreement with the 0.65 mm found above, given that the manufactured dimensions may not be exactly as drawn. The sign of the measured By vs Z is also correct for a displacement in the –y direction (given the probe coordinate system shown in Fig. 10, that Bz is negative in the model, and additional tests confirmed that the probe directions are correct).

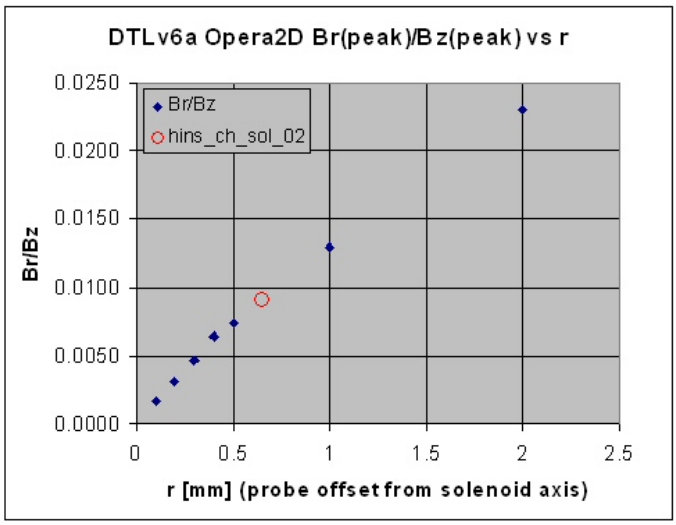

Fig. 19. Opera2D prediction for the peak Br/Bz for probe offset r from solenoid axis.

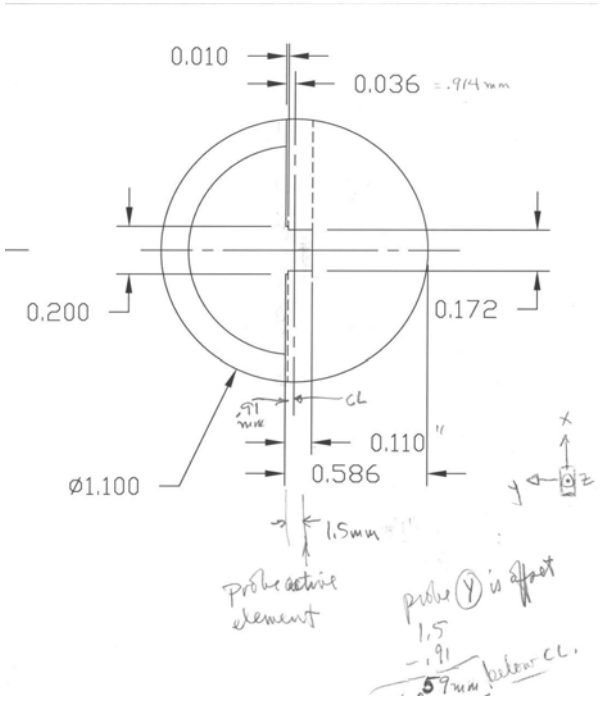

Fig. 20. G10 Hall Probe support drawing, showing dimensions relative to center line.

The corrector dipole strength and profile in Fig. 17 appear to be reasonable: one can expect a small Bz component away from the solenoid center; Bz does go to zero at the center as expected. The probe alignment along the dipole directions may not be perfect, so the difference in peak strengths of Bx and By could be due to this. Fig. 21 shows a comparison of the vector sum of transverse fields from the 3D probe with the 1D probe, scaled to the same current: these independent measurements agree reasonably well; there are some differences at the peak and positive Z tail though, which are likely the result of noisy response in the 3D probe (seen also in measurements of HINS_CH_SOL_01).

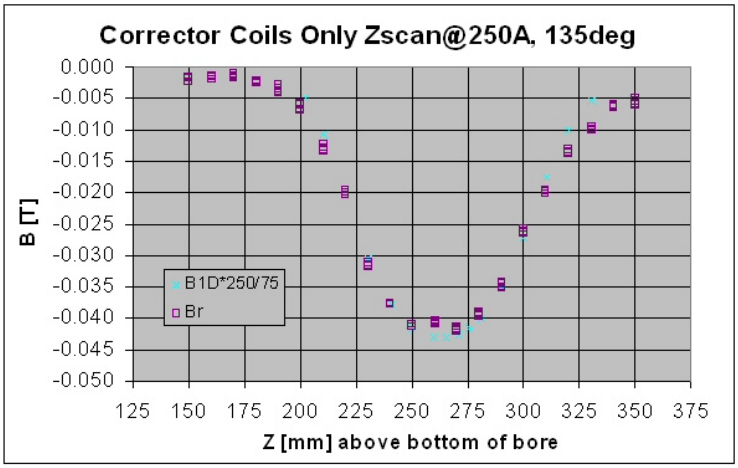

Fig. 21. Comparison of the dipole strength along the solenoid axis measured by 1D and 3D probes (where $B_r^2 = B_x^2 + B_y^2$).

IV. Conclusion

This test has shown that embedding corrector windings inside the solenoid lens can be made without compromising the performance of the lens. Even in the truncated version, the device meets criteria established for focusing elements of the initial part of the HINS linac front end. Magnetic measurements of the device reveal good agreement with expected performance, and show that the measured corrector strength is adequate. Moreover, it seems possible to use a 3D Hall probe for referencing the magnetic axis of the device to its outer surface with reasonable accuracy and precision.

References

1. G. Davis, V.V. Kashikhin, T. Page, I. Terechkine, T. Wokas, Linac CH-Type Cavity Section Focusing Solenoid Cold Mass Design, FNAL TD note TD-06-020, FNAL, 2006.
2. C. Hess, F. Lewis, D. Orris, M. Tartaglia, I. Terechkine, T. Wokas, CH Section Focusing Solenoid Cold Mass. Prototype I: HINS_CH_SOL_01. Expected Performance and Main Test Results, FNAL TD note TD-07-006, FNAL, 2007
3. G. Davis, I. Terechkine, T. Wokas, CH-Section Focusing Solenoid with Dipole Corrector Windings, FNAL TD note TD-07-001, FNAL, 2007
4. B. Wands, Summary of DTL Section Solenoid FEA, FNAL TD note TD-06-043, FNAL, 2006